

<https://helda.helsinki.fi>

---

## Temperature-Controlled Interactions between Poly(N-isopropylacrylamide) Mesoglobules Probed by Fluorescence

Fowler, Michael Andrew

2018-03-13

---

Fowler , M A , Duhamel , J , Qiu , X P , Korchagina , E & Winnik , F M 2018 , '  
Temperature-Controlled Interactions between Poly(N-isopropylacrylamide) Mesoglobules  
Probed by Fluorescence ' , Macromolecules , vol. 51 , no. 5 , pp. 1946-1956 . <https://doi.org/10.1021/acs.macromol.8b00003>

---

<http://hdl.handle.net/10138/308006>

<https://doi.org/10.1021/acs.macromol.8b00003>

---

cc\_by\_nc

acceptedVersion

---

*Downloaded from Helda, University of Helsinki institutional repository.*

*This is an electronic reprint of the original article.*

*This reprint may differ from the original in pagination and typographic detail.*

*Please cite the original version.*

# Temperature-Controlled Interactions Between Poly(*N*-isopropylacrylamide) Mesoglobules Probed by Fluorescence

Mike Fowler<sup>a</sup>, Jean Duhamel<sup>\*a</sup>

<sup>a</sup> Institute for Polymer Research, Waterloo Institute for Nanotechnology, Department of Chemistry, University of Waterloo, Waterloo, ON N2L 3G1, Canada

Xing Ping Qiu<sup>b</sup>, Evgeniya Korchagina,<sup>b</sup> Françoise M. Winnik<sup>\*b c</sup>

<sup>b</sup> Department of Chemistry, Université de Montréal, CP 6128 Succursale Centre Ville, Montréal QC H3C 3J7, Canada

<sup>c</sup> Faculty of Pharmacy and Department of Chemistry, University of Helsinki, Laboratory of Polymer Chemistry P.O.Box 55, Helsinki, FI-00014 Finland

\* To Whom correspondence should be addressed.

## ABSTRACT

The temperature-dependent behavior of aqueous solutions composed of a small amount of monodisperse poly(*N*-isopropylacrylamide) (PNIPAM) labeled at one or both ends with pyrene (Py<sub>n</sub>-PNIPAM with  $n = 1$  or  $2$ ) and a 10-fold excess of a non-fluorescent poly(*N*-isopropylacrylamide) (PNIPAM(22K),  $M_n = 22,000$  g/mol) was characterized using steady-state (SSF) and time-resolved (TRF) fluorescence. Turbidimetry studies indicated that all samples exhibited two temperature-induced transitions: one at  $T_c$ , the cloud point of the pyrene-labeled polymers and one at  $T_{c22}$ , the cloud point of PNIPAM(22K). These two transitions were also inferred from a decrease in the excimer-to-monomer fluorescence intensity ratio, namely the  $I_E/I_M$  ratio, obtained from SSF spectra. TRF decays of the pyrene monomer were acquired and fitted with a sum of exponentials to obtain the number average lifetime  $\langle \tau \rangle$ . Plots of  $\langle \tau \rangle$ -versus-temperature also showed transitions at  $T_c$  and  $T_{c22}$ . The changes in behavior observed at  $T_c$  for both  $I_E/I_M$  and  $\langle \tau \rangle$  were consistent with those observed for solutions of solely Py<sub>n</sub>-PNIPAM samples. The transitions found at  $T_{c22}$  for the Py<sub>n</sub>-PNIPAM solutions with PNIPAM(22K) were not observed in aqueous solutions of Py<sub>n</sub>-PNIPAM without PNIPAM(22K). They were explained by invoking substantial mixing of labeled and unlabeled chains as temperature exceeded  $T_{c22}$ . This mixing could only occur if the mesoglobules composed of labeled chains were not “frozen” at temperatures above  $T_{c22}$  despite forming stable entities in this temperature range. This phenomenon was rationalized by considering the difference in the characteristic reptation time of the chains found in a Py<sub>n</sub>-PNIPAM and PNIPAM(22K) mesoglobule at temperatures larger than  $T_{c22}$ .

## INTRODUCTION

Poly(*N*-isopropylacrylamide) (PNIPAM) in aqueous solution possesses a lower critical solution temperature (LCST) first reported in the late 1960s.<sup>1,2</sup> It is soluble in water at low temperatures but becomes insoluble once the temperature is raised above the cloud point ( $T_c$ ). The ability to use temperature to control the solubility of PNIPAM in water has triggered a major interest within the scientific community to characterize the interactions that take place between amphiphiles and PNIPAM, as the strength of these interactions naturally depends on the water solubility of the polymer. Amphiphilic materials investigated include hydrophobically-modified polymers,<sup>3,4</sup> surfactants,<sup>5</sup> phospholipid bilayers,<sup>6</sup> and drugs.<sup>7,8</sup> The interplay among hydrophobic substituents covalently attached to PNIPAM chains was assessed as well.<sup>9-12</sup> The disruption of hydrophobic assemblies as PNIPAM chains dehydrate and collapse around  $T_c$  has been studied experimentally and discussed from a theoretical view point to a great extent.<sup>13-21</sup>

Fluorescence spectroscopy is particularly useful to study how hydrophobes interact with each other and with the PNIPAM chain during the heat-induced phase transition of PNIPAM in water. Pyrene, a hydrophobic fluorophore, stands out as a powerful tool to study hydrophobically modified water-soluble polymers in aqueous solution.<sup>22-25</sup> The widespread use of pyrene arises from its spectroscopic properties: the high quantum yield (0.32 in cyclohexane) and long lifetime of its emission, the sensitivity of its fluorescence spectrum to the polarity of the local environment, and the ability to form an excited dimer called excimer.<sup>22-26</sup> When pyrene absorbs a photon of UV light, the excited pyrene may either fluoresce in the blue region of the visible spectrum as an isolated entity, the monomer, with a lifetime  $\tau_M$ , or it may encounter diffusionally a pyrene molecule in the ground-state and form an excited state dimer, or excimer. The excimer fluoresces in the green region of the visible spectrum with a lifetime  $\tau_{E0}$ . Pyrene excimer may also form quasi-instantaneously upon direct excitation of

assembled ground-state pyrenes.<sup>22</sup> A relative measure of the amount of excimer produced can be estimated from the ratio of the excimer-to-monomer fluorescence intensity, the  $I_E/I_M$  ratio, computed from the experimental fluorescence spectra. Information about the mode of excimer formation, either quasi-instantaneous or diffusion controlled, can be gained from the analysis of the rise time of the excimer determined from time-resolved spectra and from the wavelength of the excimer emission maximum retrieved from the fluorescence spectra.<sup>22,25,27</sup>

The photophysical properties of pyrene were exploited recently to monitor PNIPAM samples end-labeled with 1-pyrenylbutyl groups acting as hydrophobic substituents. Polymers ranging in molar mass ( $M_n$ ) from 7.6 to 44.5 kg/mol were prepared and named  $\text{Py}_n\text{-PNIPAM}$ , with  $n$  equals 1 or 2, depending on whether one or both ends of the chain were labeled with pyrene.<sup>27</sup> Because pyrene is hydrophobic (its solubility in water is  $\sim 0.7 \mu\text{M}$ ),<sup>28</sup> the  $\text{Py}_2\text{-PNIPAM}$  samples can be viewed as the fluorescent equivalents of hydrophobically-modified PNIPAM with lipophilic groups at both ends ( $\text{lip}_2\text{-PNIPAM}$ ), akin to industrially important rheology-modifiers<sup>29,30</sup> that have been studied extensively in the scientific literature by F. M. Winnik and colleagues.<sup>6,11,27,31</sup> The  $\text{Py}_n\text{-PNIPAM}$  samples were found to be faithful reporters of the aggregation below and around  $T_c$  of  $\text{lip}_2\text{-PNIPAM}$  chains in water as presented schematically later in the text (see Figure 2).<sup>27</sup> At temperatures below 15 °C,  $\text{lip}_2\text{-PNIPAM}$ s in water form polymeric flower micelles with a hydrophobic core made of the lipophilic groups stabilized by hydrated PNIPAM loops. The PNIPAM loops of the  $\text{lip}_2\text{-PNIPAM}$  micelles progressively dehydrate with increasing solution temperature until  $T_c$  is reached. The increase of solution turbidity signals the onset of inter-micellar association into larger particles named mesoglobules. The nascent mesoglobules progressively dehydrate until a temperature  $T_m$  beyond which the aggregation/dehydration processes are completed, yielding mesoglobules  $\sim 100$  to  $200$  nm in diameter, that remain colloidally stable for undefined long times with no sign of macroscopic phase separation.

Commented [JD1]: Would this be better?

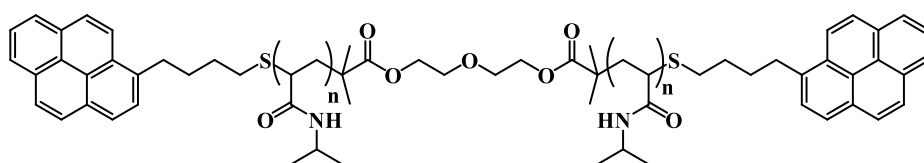
The formation of stable mesoglobules has been reported for a number of polymers in water and in organic solvents.<sup>31</sup> The properties of the mesoglobules depend on factors related to intrinsic characteristics of the polymers and to experimental protocols.<sup>15,32,33</sup> Various mechanisms have been proposed to account for the stability of mesoglobules. Electrostatic effects ascribed to low amounts of ionic species have been invoked.<sup>34</sup> Another mechanism is based on the viscoelastic effect, originally described by H. Tanaka.<sup>20,21</sup> It stipulates that a collision of two mesoglobules is effective only if their contact time is longer than the time necessary to establish permanent chain entanglements via chain reptation. In the case of PNIPAM, the mesoglobules were shown to evolve from a fluid-like particle to a “vitrified” mesoglobules when heated 6 ~ 7 °C beyond  $T_m$ .<sup>33</sup> A recent refractometry study performed on aqueous solutions of unmodified PNIPAM has questioned this claim as it found that the mesoglobules were gel-like for all temperatures above  $T_c$ .<sup>35</sup> i.e. neither glassy nor frozen, two terms often employed in the scientific literature to describe the interior of stable mesoglobules.<sup>15,20,33,35,36</sup>

The purpose of this study is to investigate the state of mesoglobules formed in aqueous solutions of semitelechelic ( $n = 1$ ) and telechelic ( $n = 2$ )  $Py_n$ -PNIPAM samples. Specifically, we prepared mixed solutions that contained a small amount of  $Py_n$ -PNIPAM with a much larger amount of unmodified PNIPAM. s. The labelled polymers varied in terms of molar mass ( $7.6 < M_n < 44.5$  kg/mol) and degree of labeling ( $n = 1$  or  $2$ ). The same unmodified polymer, PNIPAM(22K) of  $M_n = 22.0$  kg/mol, was employed in all the solutions. The cloud point,  $T_{c22}$ , of PNIPAM(22K) was higher than that of the  $Py_n$ -PNIPAM samples. Hence, the mixed solutions were expected to exhibit two cloud points, one at a constant temperature,  $T_{c22}$ , and the other at a lower temperature,  $T_c$ , characteristic of the  $Py_n$ -PNIPAM employed. Mixtures of PNIPAM(22K) and a  $Py_n$ -PNIPAM sample were prepared in two steps: the  $Py_n$ -PNIPAM chains were dissolved in cold water, which resulted in the formation of polymeric micelles,

then a solution of molecularly dissolved PNIPAM(22K) was added to the preformed polymeric micelles. These experiments were designed to assess if PNIPAM(22K) chain interact or disrupt the Py<sub>n</sub>-PNIPAM micelles in water at room temperature and to monitor the evolution of the PNIPAM(22K)/Py<sub>n</sub>-PNIPAM interactions as the solution temperature crosses  $T_c$  and  $T_{c22}$ . In most instances, mesoglobules of Py<sub>n</sub>-PNIPAM formed at temperatures lower than  $T_{c22}$ , allowing us to probe, by changes in the pyrene fluorescence, the interactions Py<sub>n</sub>-PNIPAM mesoglobules with PNIPAM(22K) as the solution temperature passed  $T_{c22}$ .

## EXPERIMENTAL

**Chemicals:** PNIPAM samples with a narrow molecular weight distribution and labeled at one or two ends with pyrene (Py<sub>n</sub>-PNIPAM(*X*) with  $n = 1$  or 2 and *X* being the number average molecular weight ( $M_n$ ) of the polymer) were synthesized according to protocols described in an earlier publication.<sup>37</sup> The chemical structure of the Py<sub>n</sub>-PNIPAM samples is shown in Figure 1. The samples used in this study, as well as their  $M_n$  and polydispersity index (PDI) values, are listed in Table 1. Unmodified PNIPAM with a molecular weight of 22 kg/mol (PNIPAM(22K)) was purchased from Sigma-Aldrich and used as received. Milli-Q water with a resistivity of over 18 MΩ·cm was used to prepare all aqueous solutions and ethanol (HPLC grade reagent alcohol) was supplied by Fischer Scientific.



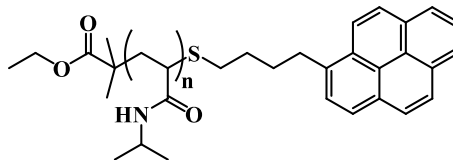


**Figure 1.** Chemical structure of (top) Py<sub>2</sub>-PNIPAM and (bottom) Py<sub>1</sub>-PNIPAM.

**Table 1:** Polydispersity index (PDI) and number average molecular weight ( $M_n$ ) of Py<sub>n</sub>-PNIPAM samples and concentration of the solutions used for fluorescence studies.

| Sample                       | $M_n$<br>(kg/mol) | PDI  | [Py <sub>n</sub> -PNIPAM]<br>(mg/L) | [PNIPAM(22K)]<br>(g/L) |
|------------------------------|-------------------|------|-------------------------------------|------------------------|
| Py <sub>2</sub> -PNIPAM(7K)  | 7.6               | 1.08 | 9.5                                 | 0.095                  |
| Py <sub>2</sub> -PNIPAM(14K) | 13.7              | 1.10 | 17.0                                | 0.17                   |
| Py <sub>2</sub> -PNIPAM(25K) | 25.4              | 1.07 | 32.0                                | 0.32                   |
| Py <sub>2</sub> -PNIPAM(45K) | 44.5              | 1.10 | 56.0                                | 0.56                   |
| Py <sub>1</sub> -PNIPAM(7K)  | 7.68              | 1.02 | 18.0                                | 0.18                   |
| Py <sub>1</sub> -PNIPAM(12K) | 12.3              | 1.02 | 30.0                                | 0.30                   |
| Py <sub>1</sub> -PNIPAM(25K) | 23.5              | 1.09 | 59.0                                | 0.59                   |
| PNIPAM(22K)                  | 20-25             |      |                                     |                        |

*Preparation of aqueous solutions of Py<sub>n</sub>-PNIPAM and PNIPAM(22K):* Aqueous mixtures of PNIPAM(22K) and the Py<sub>n</sub>-PNIPAM samples were prepared by dissolving the Py<sub>n</sub>-PNIPAM samples in ethanol, determining the concentration of this solution by applying the Beer-Lambert law to the absorbance of pyrene at 344 nm with the molar absorbance coefficient of 1-pyrenebutanol in ethanol ( $\epsilon_{Py}(344 \text{ nm}) = 42,500 \text{ M}^{-1} \cdot \text{L} \cdot \text{cm}^{-1}$ ), then transferring a sufficient quantity into a vial that would yield the desired concentration in a given volume of water. The ethanol was evaporated under a stream of nitrogen. The use of ethanol was required to avoid



errors in concentrations due to the hypochromicity of Py derivatives in water. The residual polymer was dissolved in 0.2 mL of water. The vial was vortexed, 0.8 mL of water was added, and the solution was vortexed again. A known mass of PNIPAM(22K) was dissolved in water to yield a stock solution which was diluted to the desired concentration. This PNIPAM(22K) solution (3 mL) was added to the 1 mL  $\text{Py}_n$ -PNIPAM aqueous solution to yield a mixture with a known concentration of  $\text{Py}_n$ -PNIPAM, and a PNIPAM(22K) massic concentration in g/L equal to 10 $\times$  that of  $\text{Py}_n$ -PNIPAM. The mixture was allowed to stand for a minimum of 30 minutes at 4 °C. Solutions composed solely of unlabeled PNIPAM were prepared by diluting the PNIPAM(22K) stock solution. Polymer solutions were prepared with a constant pyrene concentration of 2.5  $\mu\text{M}$ , resulting in  $\text{Py}_n$ -PNIPAM and PNIPAM(22K) solutions whose concentrations have been listed in Table 1.

*Steady-state fluorescence:* All fluorescence spectra were acquired with a Photon Technology International (PTI) steady-state fluorometer. The fluorescence measurements aiming to characterize the behavior of the hydrophobic pyrene labels were conducted in the dilute regime with massic concentrations lower than 60 mg/L for all  $\text{Py}_n$ -PNIPAM samples. To monitor the state of the polymer solutions as their temperature passed through  $T_c$  and  $T_{c22}$ , the cloud point temperature of the  $\text{Py}_n$ -PNIPAM and PNIPAM(22K) samples, respectively, the light scattered by the solutions was monitored with the fluorometer by exciting the solutions at 500 nm where pyrene does not absorb and measuring the emission intensity from 490 to 510 nm in 0.5 nm increments. These experiments were carried out as a function of temperature with 1 °C increments, waiting 10 minutes before measurements to record the intensity of scattered light. The light scattering (LS) intensity was integrated and plotted as a function of temperature. The LS intensity was monitored as a function of temperature up to 40 °C when the solution was cooled to 20 °C and a second heating ramp was applied to the solutions to probe whether sample history had an effect on the solution behavior. The absolute LS intensity was difficult to control

between runs on different days as it depended on the specific settings of the fluorometer (monochromator slit widths, lamp intensity, etc...) applied on each run and consequently, could not be directly compared between samples. The LS intensity profiles corresponding to the 1<sup>st</sup> and 2<sup>nd</sup> heating ramps were conducted on a same day however and could be compared.

The fluorescence spectra, that monitored the behavior of the pyrene hydrophobes, were acquired from 350 to 600 nm by exciting the solution at 342 nm. They were analyzed to obtain the monomer ( $I_M$ ) and excimer ( $I_E$ ) fluorescence intensities that were used to calculate the  $I_E/I_M$  ratio which is a measure of the efficiency of the sample at forming excimer.  $I_M$  was typically determined by integration of the fluorescence spectrum from 372 to 378 nm which corresponds to the 0-0 transition of pyrene in the fluorescence spectrum.  $I_E$  was obtained by subtracting the fluorescence spectrum of the Py<sub>1</sub>-PNIPAM(25K) sample acquired at the same temperature from the spectrum of a given Py<sub>2</sub>-PNIPAM construct after normalization at the 0-0 transition. The Py<sub>1</sub>-PNIPAM(25K) sample was selected for this purpose as it generated hardly any excimer.<sup>27</sup> The trace obtained after subtraction was integrated from 420 to 600 nm to obtain  $I_E$ . This procedure has been described in detail in an earlier publication<sup>27</sup> and it was applied to the Py<sub>2</sub>-PNIPAM samples due to the shift of the excimer fluorescence observed at temperatures greater than  $T_c$ . The fluorescence spectra were also analyzed to obtain the wavelength ( $\lambda_{max}$ ) corresponding to the maximum of the excimer fluorescence intensity. To this end, the fluorescence spectra were fitted with a polynomial between 435 to 535 nm. The derivative of the polynomial with respect to wavelength was determined and the wavelength where the derivative equaled zero was selected as  $\lambda_{max}$ . Since the excimer fluorescence maximum of the Py<sub>1</sub>-PNIPAM samples did not shift with temperature,  $I_M$  and  $I_E$  were determined by taking the integral under the fluorescence signal from 372 to 378 nm and from 500 to 530 nm, respectively.

*Time-resolved fluorescence:* The fluorescence decays were acquired with an IBH time-resolved fluorometer using a 340 nm nanoLED as the excitation source. The Py<sub>n</sub>-PNIPAM aqueous solutions were excited at 342 nm with the excitation monochromator and their emission was monitored at 375 nm with a 370 nm cut-off filter for the monomer fluorescence decay acquisition. The cut-off filter was used to minimize stray scattered light from reaching the detector. The pyrene monomer fluorescence decays were fitted with a sum of exponentials using Eq. 1.

$$i(t) = a_1 \exp(-t/\tau_1) + a_2 \exp(-t/\tau_2) + a_3 \exp(-t/\tau_3) \quad (1)$$

The variables  $a_i$  and  $\tau_i$  in Eq. 1 refer to the  $i^{\text{th}}$  pre-exponential factor and decay time, respectively, obtained from the multi-exponential fit of the decays and are provided as Supporting Information (SI). They were optimized by using the Marquardt-Levenberg algorithm.<sup>38</sup> Eq. 2 was used to calculate the number-average lifetime  $\langle \tau \rangle$  of the fluorescence decays of the pyrene monomer.

$$\langle \tau \rangle = \frac{\sum a_i \tau_i}{\sum a_i} \quad (2)$$

Excimer fluorescence decays were also acquired but their quantitative analysis was complicated by a short rise time that overlapped with a short decay component at the early times that was attributed to residual LS despite the use of cut-off filters. These complications were expected since the excimer fluorescence signal decreased dramatically for all Py<sub>n</sub>-PNIPAM samples at temperatures larger than  $T_m$ . Consequently, the results obtained from the analysis of the excimer fluorescence decays were not discussed herein.

## RESULTS AND DISCUSSION

The experiments presented hereafter were performed on solutions set initially at 20 °C, a temperature for which PNIPAM(22K) is soluble and the labeled chains form polymeric rosette micelles with a hydrophobic core stabilized by soluble PNIPAM loops. The only exception to this protocol was the case of mixed Py<sub>2</sub>-PNIPAM(7K)/PNIPAM(22K) solutions for which the initial temperature was set at 15 °C, since Py<sub>2</sub>-PNIPAM(7K) is not soluble in water at 20 °C. The temperature was then increased in small increments, typically 1 °C, with a minimum equilibration time of 10 minutes before performing fluorescence measurements until the temperature reached 40 °C, a temperature where the two water-insoluble polymers may form mixed mesoglobules, but only if the Py<sub>n</sub>-PNIPAM mesoglobules formed at  $T_c$  are neither gel-like. Subsequently, in some cases, the mixed solutions were cooled to 20 °C at a maximum cooling rate of 0.5 °C per minute to redissolve the polymer. The solutions were re-heated from 20 to 40 °C under the same conditions to determine if the thermal history of the samples affects the association of the labeled chains below  $T_c$ . There were no significant difference in the trends observed in the 1<sup>st</sup> and 2<sup>nd</sup> heating ramps.

**Characterization of the Py<sub>n</sub>-PNIPAM – PNIPAM(22K) mixtures by light scattering.** The  $T_c$  values of the mixed solutions were determined from the changes with temperature of the intensity of the light scattered by the solutions, as described in details in Supporting Information (SI). All LS intensity vs temperature profiles obtained for the mixed Py<sub>2</sub>-PNIPAM/PNIPAM(22K) samples present a transition at 33 °C, attributed to the dehydration of PNIPAM(22K). This temperature is designated  $T_{c22}$  in the following. The traces feature a second transition ranging from 20 to 29 °C with increasing molar mass in the case of the telechelic Py<sub>2</sub>-PNIPAM samples. In the case of the semitelechelic Py<sub>1</sub>-PNIPAM samples,  $T_c$  takes the same value, 30 °C, regardless of  $M_n$ . Interestingly, the  $T_c$  values of Py<sub>n</sub>-PNIPAM in mixed solutions are identical, within experimental uncertainty, to the  $T_c$  of the labeled polymers

aqueous solutions in the absence PNIPAM(22K).<sup>27</sup> The fact that the presence of PNIPAM(22K) has little effect on the cloud point of Py<sub>n</sub>-PNIPAM suggests that the dehydration of PNIPAM(22K) at 33 °C and the hydrophobic collapse observed for the Py<sub>n</sub>-PNIPAM samples at  $T_c$  take place independently of each other. Table 2 summarizes the  $T_c$  values obtained by LS with the Py<sub>n</sub>-PNIPAM solutions with or without PNIPAM(22K).

**Table 2.**  $T_c$  values of the Py<sub>2</sub>-PNIPAM samples

| Sample                                      | $T_c$ (°C), with 10-fold excess PNIPAM(22K) <sup>a</sup> | $T_c$ (°C), without PNIPAM(22K) <sup>27</sup> |
|---|--|---|
| Py <sub>2</sub> -PNIPAM(7K)                 | 20   | 22  |
| Py <sub>2</sub> -PNIPAM(14K)                | 24   | 25  |
| Py <sub>2</sub> -PNIPAM(25K)                | 28   | 28  |
| Py <sub>2</sub> -PNIPAM(45K)                | 29   | 28  |
| Py <sub>1</sub> -PNIPAM(7-25K) <sup>b</sup> | 30   | 30  |

a:  $T_{c22}$  for PNIPAM(22K) = 33 °C.

b: all Py<sub>1</sub>-PNIPAM samples have the same turbidity profiles.

An earlier examination of the pyrene excimer fluorescence of aqueous Py<sub>n</sub>-PNIPAM samples without excess PNIPAM(22K) led to the conclusion that all Py<sub>n</sub>-PNIPAM samples form glassy mesoglobules around 33 °C, the value corresponding to  $T_{c22}$ , which is higher than  $T_c$  of the respective Py<sub>n</sub>-PNIPAM samples.<sup>27</sup> In mixed solutions where the  $T_c$  of Py<sub>2</sub>-PNIPAM is lower than  $T_{c22}$ , the dehydration of PNIPAM(22K) could lead to the mixing of the two polymers once the solution temperature reaches 33 °C, but only if the Py<sub>2</sub>-PNIPAM mesoglobules are not frozen. As the fluorescence of the pyrene labels of Py<sub>2</sub>-PNIPAM samples is very sensitive to changes in the pyrene environment, it is ideally suited to determine

experimentally whether or not mesoglobules mixing occurs in mixed  $\text{Py}_n$ -PNIPAM/PNIPAM(22K) solutions.

***Temperature-dependence of the steady-state fluorescence of  $\text{Py}_n$ -PNIPAM/PNIPAM(22K)***

***mixtures.*** In order to distinguish the spectral features intrinsic to  $\text{Py}_2$ -PNIPAM from the indirect effects induced by the excess PNIPAM in solution, it is useful to recall the features of the fluorescence spectra acquired for  $\text{Py}_2$ -PNIPAM solutions without added PNIPAM<sup>27</sup> and to compare them with the results of this study. As seen in Figure 2, which presents the spectra of  $\text{Py}_2$ -PNIPAM(14K) without PNIPAM (top) and with PNIPAM (bottom), an increase in the solution temperature from 20 °C up to the cloud point of the solution leads to an increase in the relative amount of excimer formed by  $\text{Py}_2$ -PNIPAM(14K). The excimer emission enhancement is seen in both cases. It is attributed to the shrinkage of the micelles as a result of the dehydration of the PNIPAM segments that brings the pyrene labels closer to each other.<sup>27</sup> At temperatures higher than  $T_c$ , the amount of excimer generated by  $\text{Py}_2$ -PNIPAM(14K) starts to decrease with increasing temperature. This effect corresponds to the formation of mesoglobules and concomitant reduction of the pyrenes mobility. In the case of  $\text{Py}_2$ -PNIPAM(14K) samples without PNIPAM(22K), the excimer emission intensity reaches a plateau value as the solution temperature reached  $\sim 33$  °C, a value similar to  $T_{c22}$  (Figure 2, top). In contrast, increasing the temperature past  $T_{c22}$  for solutions of  $\text{Py}_2$ -PNIPAM(14K) in the presence of PNIPAM(22K) results in an abrupt decrease in excimer intensity (Figure 2, bottom). A similar behavior was observed for all mixed  $\text{Py}_2$ -PNIPAM solutions.

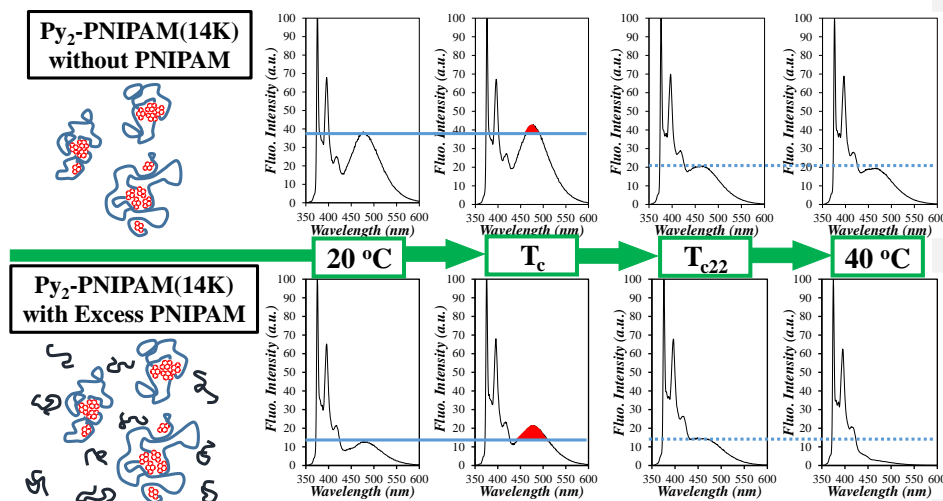


**Figure 2.** Comparison of the behavior exhibited by the fluorescence spectra of Py<sub>2</sub>-PNIPAM(14K) in water without (top panel) and with (bottom panel) 10-fold excess PNIPAM(22K). The solid and dashed blue lines help to identify the difference in relative excimer fluorescence intensity when the solution temperature is increased from 20 °C to T<sub>c</sub> and from T<sub>c22</sub> to 40 °C, respectively.

Fluorescence spectra of Py<sub>2</sub>-PNIPAM(14K) with a 10-fold excess of PNIPAM(22K), normalized at the 0-0 transition of pyrene (375 nm) and their changes as the solution temperature increases in 1 °C increments are shown in Figures 3A-C. This representation allows one to visualize the changes in excimer fluorescence, relative to the monomer emission intensity. The relative excimer emission intensity increases with increasing solution temperature as it approaches T<sub>c</sub>, and it decreases upon further increase of the solution temperature. Of particular interest is the significant and continuous drop in excimer fluorescence intensity as the solution exceeds T<sub>c22</sub>, the cloud point temperature of PNIPAM(22K). Since this drop in excimer fluorescence intensity does not occur in the absence of PNIPAM(22K) (Figure 2, top),<sup>27</sup> it is reasonable to conclude that the excimer disappearance

above  $T_{c22}$  results from interactions between isolated pyrene labels and the dehydrated PNIPAM(22K) chains.

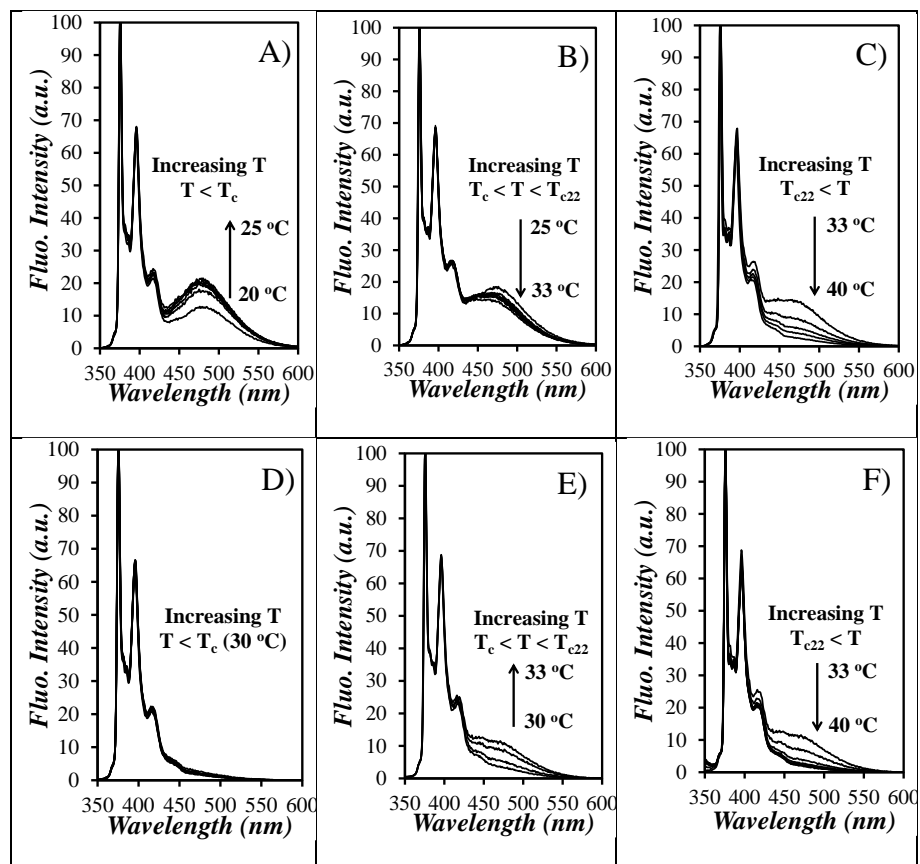


**Figure 3.** Steady-state fluorescence spectra of aqueous mixtures of PNIPAM(22K) and Py<sub>2</sub>-PNIPAM(14K) for temperatures increasing from A) 20 to 25 °C ( $T_c$ ), B) 25 ( $T_c$ ) to 33 °C ( $T_{c22}$ ), and C) 33 ( $T_{c22}$ ) to 40 °C, and Py<sub>1</sub>-PNIPAM(7K) for temperatures increasing from D) 20 to 30 °C ( $T_c$ ), E) 30 ( $T_c$ ) to 33 °C ( $T_{c22}$ ), and F) 33 ( $T_{c22}$ ) to 40 °C.

The fluorescence spectra of the Py<sub>2</sub>-PNIPAM(14K) samples shown in Figures 3A-C provide a qualitative representation of the temperature dependence of the excimer fluorescence intensity. The ratio  $I_E/I_M$ , calculated from the spectra, yields a more quantitative representation



of the effects. The changes with temperature of the ratio  $I_E/I_M$  for the four Py<sub>2</sub>-PNIPAM/PNIPAM(22K) mixed solutions are plotted in Figure 4. All samples experience an increase in  $I_E/I_M$  with increasing temperature up to  $T_c$ , at which points the ratio decreases at first sharply over a narrow temperature window, then more gradually until the temperature reaches  $T_{c22}$ . Above this temperature,  $I_E/I_M$  undergoes a second sharp decrease. These trends were observed for mixed solutions of Py<sub>2</sub>-PNIPAM(7K), Py<sub>2</sub>-PNIPAM(14K), and Py<sub>2</sub>-PNIPAM(25K). In the case of Py<sub>2</sub>-PNIPAM(45K) the  $I_E/I_M$  ratio shows a single transition at  $T_c$  (see Figure 4B, which presents an expanded view of the data). This polymer does not form micelles in water at room temperature. The excimer emission is weak throughout the temperature range probed here, such that the minor changes in  $I_E/I_M$  cannot be detected reliably. In Figure 4B, we present the temperature variation of  $I_E/I_M$  recorded for two successive heating ramps (full symbol: 1st heating, open symbol: 2<sup>nd</sup> heating) in the case of Py<sub>2</sub>-PNIPAM(14K) and Py<sub>2</sub>-PNIPAM(25K) mixed solutions. The two curves are nearly identical, hence upon cooling, the solutions recover their original state, without change in either  $T_c$  or  $T_{c22}$ .

Several events may account for the massive decrease in  $I_E/I_M$  observed at  $T_c$  and  $T_{c22}$  for all Py<sub>2</sub>-PNIPAM samples (Figure 4). A decrease in the mobility of pyrene, its accessibility to the solvent, or its local concentration in the mesoglobules can result in a decrease of the Py excimer emission. Separation of the pyrenes as the Py<sub>2</sub>-PNIPAM micelles dehydrate and assemble in mesoglobules reduces the probability of pyrene-pyrene encounters, hence decreases the probability of diffusive excimers formation. It also precludes the formation of ground-state pyrene aggregates which upon direct excitation would form excimer instantaneously. A decrease in mobility of the pyrene labels would affect their ability to diffuse and encounter each other, thus reducing pyrene excimer formation. Shielding pyrene from oxygen dissolved in water, a powerful quencher of pyrene fluorescence, would increase the

quantum yield of pyrene and result in a larger  $I_M$  that would reduce the  $I_E/I_M$  ratio. A priori, the decrease in  $I_E/I_M$  observed at  $T_c$  can result from

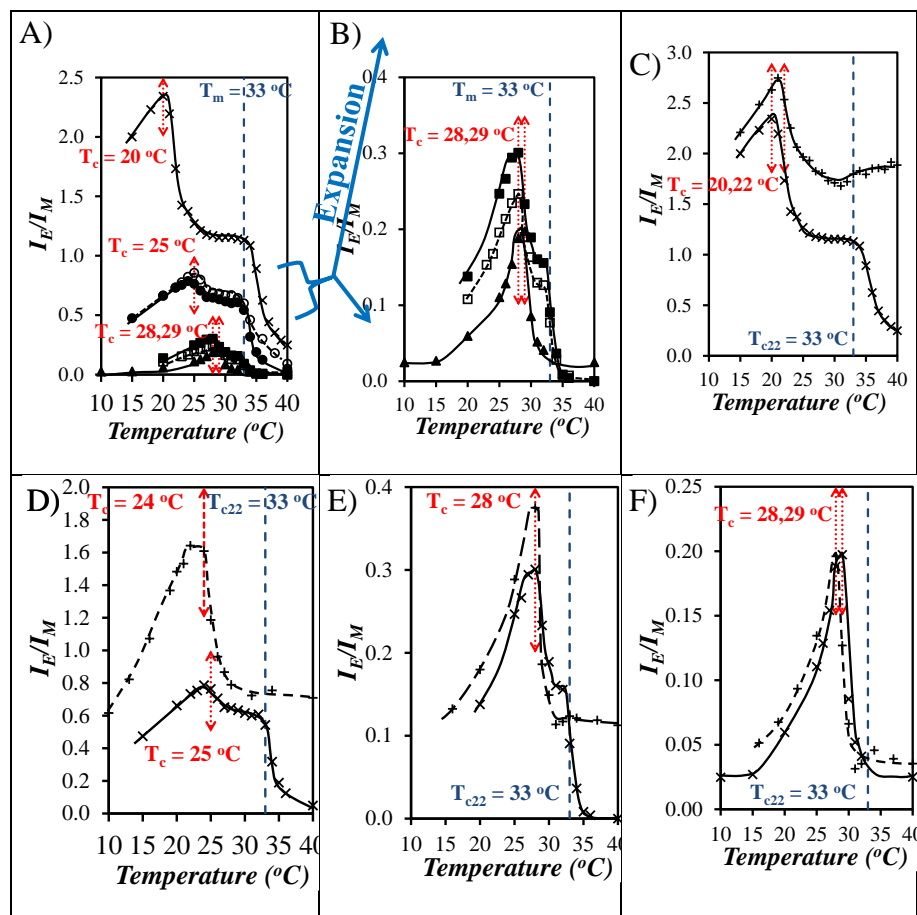


**Figure 4:** Plots of the  $I_E/I_M$  ratio for aqueous mixtures of Py<sub>2</sub>-PNIPAM and PNIPAM(22K) as

a function of solution temperature. A) (×) Py<sub>2</sub>-PNIPAM(7K), (●, ○) Py<sub>2</sub>-PNIPAM(14K), (■, □) Py<sub>2</sub>-PNIPAM(25K), and (▲) Py<sub>2</sub>-PNIPAM(45K). B) Expanded view of Py<sub>2</sub>-PNIPAM(25K) and Py<sub>2</sub>-PNIPAM(45K). Comparison of C) Py<sub>2</sub>-PNIPAM(7K), D) Py<sub>2</sub>-PNIPAM(14K), E) Py<sub>2</sub>-PNIPAM(25K), and F) Py<sub>2</sub>-PNIPAM(45K) with (×) and without (+) a 10 fold excess of PNIPAM(22K). open symbols: 2<sup>nd</sup> heating ramp.

a combination of all these effects as they are all expected to occur upon mesoglobule formation. However, an earlier study<sup>27</sup> has shown that the kinetics of pyrene excimer formation do not change significantly at 33 °C ( $T_{c22}$ ) in the absence of unlabeled PNIPAM. Plots of  $I_E/I_M$  versus temperature for Py<sub>2</sub>-PNIPAM samples without (data points represented by: +) and with (data points represented by: x) a 10-fold excess of PNIPAM(22K) are presented in Figures 4C-F). The  $I_E/I_M$  values recorded for Py<sub>2</sub>-PNIPAM solutions without added PNIPAM(22K) remain nearly constant at temperatures higher than  $T_c + \sim 4$  °C (i.e after the initial sharp decrease of  $I_E/I_M$ ) up to 40 °C, The precipitous decrease of  $I_E/I_M$  at  $T_{c22}$  observed in mixed solutions must be ascribed to interactions between dehydrated and collapsed PNIPAM(22K) and Py<sub>2</sub>-PNIPAM mesoglobules.

From the curves shown in Figures 4C-E one observes also that the  $I_E/I_M$  ratios recorded in mixed solutions for  $T < T_{c22}$  are smaller than the  $I_E/I_M$  ratios obtained for solutions of pure Py<sub>2</sub>-PNIPAM, at least in the case of the shorter labeled polymers (Figure 4C-D). The relatively low  $I_E/I_M$  in mixed solutions reflects some level of interactions between Py<sub>2</sub>-PNIPAM micelles and PNIPAM(22K) in mixed solutions kept at  $T < T_{c22}$ .

Pyrene aggregates are known to absorb light less effectively than single pyrenes forming excimer through diffusive encounters.<sup>39,40</sup> This effect may also account for the decrease of  $I_E$ , and consequently  $I_E/I_M$ , at  $T_c$  and  $T_{c22}$ . Changes in excimer stacking can be inferred from a shift in the wavelength of maximum emission ( $\lambda_{max}$ ). A blue-shift in emission corresponds to overall higher levels of pyrene aggregation.<sup>27</sup> The  $\lambda_{max}$  values, calculated by fitting the excimer fluorescence spectra with a polynomial and finding mathematically the wavelength corresponding to its maximum, are presented in Figure 5. They display a sharp blue-shift around the respective  $T_c$ , of each Py<sub>2</sub>-PNIPAM, implying a significant change in the mechanism of excimer formation at  $T_c$ . A blue shift in excimer fluorescence is usually

attributed to a switch in excimer formation from diffusive encounters between pyrene labels to direct excitation of pyrene aggregates.<sup>22,27</sup> The decrease in excimer formation observed (Figure 4) at  $T_c$  for each Py<sub>2</sub>-PNIPAM sample and associated with the blue shift in excimer fluorescence also occurs also at  $T_c$  as shown in Figure 5. This coincidence suggests that the formation of mesoglobules by the Py<sub>2</sub>-PNIPAM samples at  $T_c$  leads to a reduction in excimer formation by diffusion consistent with a reduction in pyrene mobility.

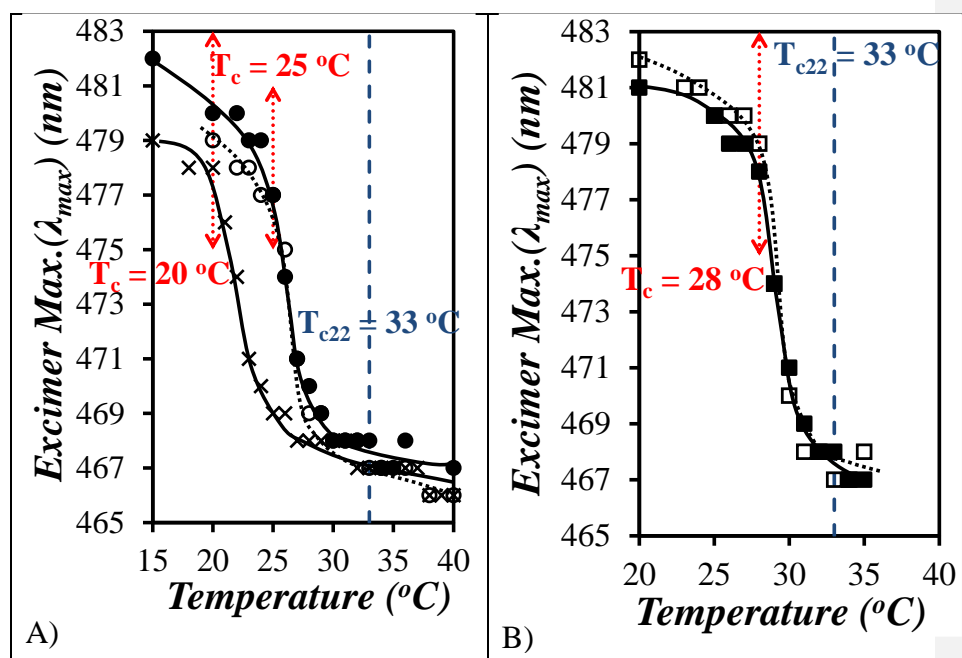


**Figure 5.** Plots of the maximum wavelength of excimer fluorescence for aqueous mixtures of

Py<sub>2</sub>-PNIPAM and PNIPAM(22K) as a function of solution temperature. A) (  $\times$  ) Py<sub>2</sub>-PNIPAM(7K), (  $\bullet$ ,  $\circ$  ) Py<sub>2</sub>-PNIPAM(14K) and B) (  $\blacksquare$ ,  $\square$  ) Py<sub>2</sub>-PNIPAM(25K). open symbols: 2<sup>nd</sup> heating ramp. The absence of sufficiently strong excimer fluorescence intensity across the entire temperature range (20 – 40 °C) and between 35 and 40 °C for, respectively, for the Py<sub>2</sub>-PNIPAM(45K) and Py<sub>2</sub>-PNIPAM(25K) samples led to the dismissal for  $\lambda_{max}$

determination at all temperatures for Py<sub>2</sub>-PNIPAM(45K) and at temperatures above 35 °C for Py<sub>2</sub>-PNIPAM(25K).

Further heating of Py<sub>2</sub>-PNIPAM(7K) and Py<sub>2</sub>-PNIPAM(14K) samples above  $T_c$  has no significant effect on  $\lambda_{\max}$  : it decreases slightly with increasing temperature up to 40 °C, with no significant change at  $\sim T_{c22}$ . Based on the trends obtained with the Py<sub>2</sub>-PNIPAM samples which showed sufficient excimer formation at  $T > T_c$ , the absence of a shift in  $\lambda_{\max}$  at  $T_{c22}$  (= 33 °C) implies that the decrease in  $I_E/I_M$  at  $T_{c22}$  observed in Figure 4 corresponds to a decrease in the number of excimer-forming pyrenes, probably due to their dilution within mesoglobules formed upon dehydration of PNIPAM(22K).

We now turn to the properties of mixed solutions of the semitelechelic Py<sub>1</sub>-PNIPAM samples and PNIPAM(22K). Fluorescence spectra of mixed Py<sub>1</sub>-PNIPAM(7K)/PNIPAM(22K) heated from 20 and 40 °C are presented in Figures 3D-F. Spectra recorded from 20 to 30 °C, (Figure 3D) feature exclusively emission from Py monomer. As the temperature exceeds 30 °C, the  $T_c$  of Py<sub>1</sub>-PNIPAM(7K), excimer fluorescence appears and it increases with increasing temperature up to 33 °C ( $T_{c22}$ ) (Figure 3E), then upon further heating the excimer fluorescence decreases (Figure 3F). The corresponding changes in the  $I_E/I_M$  ratio are presented in Figure 6. In all cases,  $I_E/I_M$  increases slightly with increasing temperature in the low temperature regime ( $< T_c$ ). It undergoes a sharp increase at  $T_c = 30$  °C, reflecting the increase in local pyrene concentration as the Py<sub>1</sub>-PNIPAM chains collapse and aggregate. The  $I_E/I_M$  ratio passes through a maximum at  $T_{c22} = 33$  °C. The fact that  $I_E/I_M$  decreases with increasing temperature once the solution had reached  $T_{c22}$  implies that dehydrated PNIPAM(22K) and Py<sub>1</sub>-PNIPAM interact. In the absence of PNIPAM(22K) (Figure 6D, symbols: +),  $I_E/I_M$  does not decrease. It increases smoothly from  $T_c$  (= 30 °C) to 40 °C. The contrasting trends of  $I_E/I_M$  shown in Figure 6D provide strong evidence that in

mixed solutions of  $T > T_{c22}$ , the dehydrated PNIPAM(22K) chains associate with the Py<sub>1</sub>-PNIPAM mesoglobules, resulting in the dilution of the pyrenyl pendants in the hydrophobic PNIPAM matrix and the associated decrease in  $I_E/I_M$ . Here again, the extensive mixing happening between the Py<sub>1</sub>-PNIPAM mesoglobules and PNIPAM(22K) suggests that the Py<sub>1</sub>-PNIPAM mesoglobules are not kinetically frozen at temperatures above  $T_c$  at least up to 40 °C.

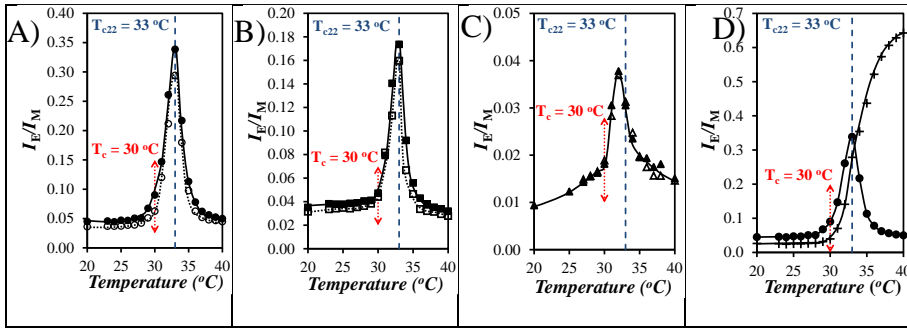


**Figure 6.** Plots of  $I_E/I_M$  for aqueous mixtures of Py<sub>1</sub>-PNIPAM and PNIPAM(22K) as a function of solution temperature. A) (●,○) Py<sub>1</sub>-PNIPAM(7K), B) (■,□) Py<sub>1</sub>-PNIPAM(12K), C) (▲,△) Py<sub>1</sub>-PNIPAM(25K), and D) Py<sub>1</sub>-PNIPAM(7K) with (●) and without (⊕) PNIPAM(22K). Hollow symbols: 2<sup>nd</sup> heating ramp.

**Behavior of the Py<sub>n</sub>-PNIPAM – PNIPAM(22K) mixtures characterized by time-resolved fluorescence:** Time-resolved fluorescence decays of the pyrene monomer were acquired for mixed solutions and fitted with Eq. 1. The parameters retrieved from the fits were used to calculate the average pyrene monomer lifetimes  $\langle \tau \rangle$  using Eq. 2. Plots of  $\langle \tau \rangle$  as a function of temperature are presented in Figure 7 for three Py<sub>2</sub>-PNIPAM samples. In mixed Py<sub>2</sub>-PNIPAM(14K)/PNIPAM(22K) solutions, Figure 7B,  $\langle \tau \rangle$  increases sharply, first for  $T = T_c$  and, second, for  $T = T_{c22}$ . In the case of Py<sub>2</sub>-PNIPAM(7K), Figure 7A, a single transition is observed for  $T = T_{c22}$ , whereas in the case of Py<sub>2</sub>-PNIPAM(25K) one observes a sharp transition at  $T_c$  ( $= 28$  °C) and a weak shoulder around  $T_{c22}$  (Figure 7C). Two consecutive heating/cooling

ramps were implemented for the Py<sub>2</sub>-PNIPAM(14K) and Py<sub>2</sub>-PNIPAM(25K) samples. The  $\langle \tau \rangle$  values obtained in the two treatments did not overlap perfectly, but their trends were quite similar and featured two transitions (at  $T_c$  and  $T_{c22}$ ).

The increase in  $\langle \tau \rangle$  observed with the mixed Py<sub>2</sub>-PNIPAM/PNIPAM-22K samples either at  $T_c$  or  $T_{c22}$  correspond to a decrease in the rate of diffusional excimer formation, which may be attributed to a stiffening of the mesoglobule matrix, a decrease in the local pyrene concentration, a decrease in the efficiency of oxygen quenching which increased  $\langle \tau \rangle$ , or a combination of all three factors. These effects can result from the collapse of the PNIPAM segments of Py<sub>2</sub>-PNIPAM samples at  $T_c$  and/or their collapse of PNIPAM(22K) at  $T_{c22}$ . While the transition in  $\langle \tau \rangle$  values at  $T_c$  may reasonably be influenced by a change in the rate of excimer formation, as seen in an earlier report,<sup>27</sup> there is less evidence to support such an explanation for the change in  $\langle \tau \rangle$  that occurred at  $T_{c22}$ . Indeed,  $\langle \tau \rangle$  remained more or less constant with temperature above  $T_{c22}$  for all Py<sub>n</sub>-PNIPAM solutions without PNIPAM(22K) (see grey symbols in Figures 7A-C). Both the increased amount of isolated pyrene monomers and the decreased oxygen quenching efficiency at  $T_{c22}$  can result from the merging of Py-PNIPAM and PNIPAM(22C) at  $T_{c22}$  which causes the dilution of isolated pyrenes in the dehydrated PNIPAM matrix and hinders diffusive encounters of pyrenes.

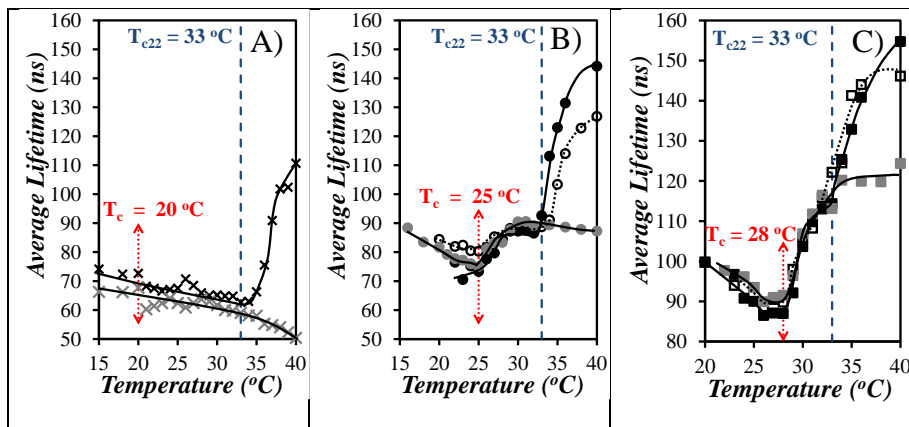


**Figure 7.** Plots of  $\langle \tau \rangle$  for pyrene monomer decays for aqueous Py<sub>2</sub>-PNIPAM / PNIPAM(22K) mixtures as a function of solution temperature. A) (  $\times$  ) Py<sub>2</sub>-PNIPAM(7K), B) (  $\bullet$ ,  $\circ$  ) Py<sub>2</sub>-PNIPAM(14K), and C) (  $\blacksquare$ ,  $\square$  ) Py<sub>2</sub>-PNIPAM(25K). Hollow symbols: 2<sup>nd</sup> heating ramp. Grey symbols: Py<sub>2</sub>-PNIPAM aqueous solutions without PNIPAM(22K).<sup>27</sup>

Comparing Figure 7 and Figure 4C-E, we observe that the trends of  $\langle \tau \rangle$  vs T obtained for mixed Py<sub>2</sub>-PNIPAM/PNIPAM(22K) solutions and Py<sub>2</sub>-PNIPAM alone are nearly identical at  $T < T_{c22}$ , whereas the changes in  $I_E/I_M$  vs T show substantial differences for the two types of solutions. Since the lifetime measurements conducted on the pyrene monomer reflect only pyrene excimer formation by diffusion, while the  $I_E/I_M$  ratios report on pyrene excimer formation by both diffusive encounters between pyrene labels and direct excitation of pyrene aggregates, we conclude that the smaller  $I_E/I_M$  ratios observed for  $T < T_{c22}$ , combined with the similarity of the  $\langle \tau \rangle$  trends, are due to the decrease in relative pyrene aggregation in mixed solutions.

Trends in  $\langle \tau \rangle$  recorded for mixed solutions of the semi-telechelic samples Py<sub>1</sub>-PNIPAM samples are presented in Figure 8. The value of  $\langle \tau \rangle$  remains nearly constant ( $104 \pm 4$  ns) in solutions warmed between 20 °C and  $T_{c22}$ . It increases sharply over a narrow



temperature window around  $T_{c22}$ , and reaches a constant value ( $144 \pm 5$  ns) in solutions heated past 36 °C. From the lack of response of  $\langle \tau \rangle$  at  $T_c = 30$  °C for all three Py<sub>1</sub>-PNIPAM samples although excimer emission takes place at this temperature (Figure 6), we conclude that the Py<sub>1</sub>-PNIPAM mesoglobules formation at  $T_c$  does not affect significantly the efficiency of oxygen quenching. In contrast, the oxygen quenching efficiency is affected for  $T > T_{c22}$  in mixed solutions of PNIPAM(22K) and either Py<sub>1</sub>-PNIPAM(7K) or Py<sub>1</sub>-PNIPAM(12K). Therefore it is reasonable to assume that the similarities in decay times observed for the Py<sub>1</sub>-PNIPAM samples around  $T_{c22}$  in Figure 8 are the result of changes in the environment of the pyrene labels upon interaction with PNIPAM(22K) mesoglobules, which lead to a reduction in oxygen quenching and a lengthening of  $\langle \tau \rangle$ . The  $\langle \tau \rangle$  vs T profiles obtained for Py<sub>1</sub>-PNIPAM(25K) with or without 10-fold excess PNIPAM(22K) were identical, presumably because the PNIPAM content in this sample is sufficiently ample to create on its own an efficient barrier against oxygen quenching for the relatively few Py groups linked to the chain ends. The shorter Py<sub>1</sub>-PNIPAM samples required mixing with PNIPAM(22K) to ensure protection against oxygen quenching resulting in the observed increase in  $\langle \tau \rangle$  at  $T_{c22}$ . Evidence of mixing between the Py<sub>1</sub>-PNIPAM(25K) mesoglobules and PNIPAM(22K) is drawn from the decrease in  $I_E/I_M$  observed at  $T_{c22}$  in Figure 6C.

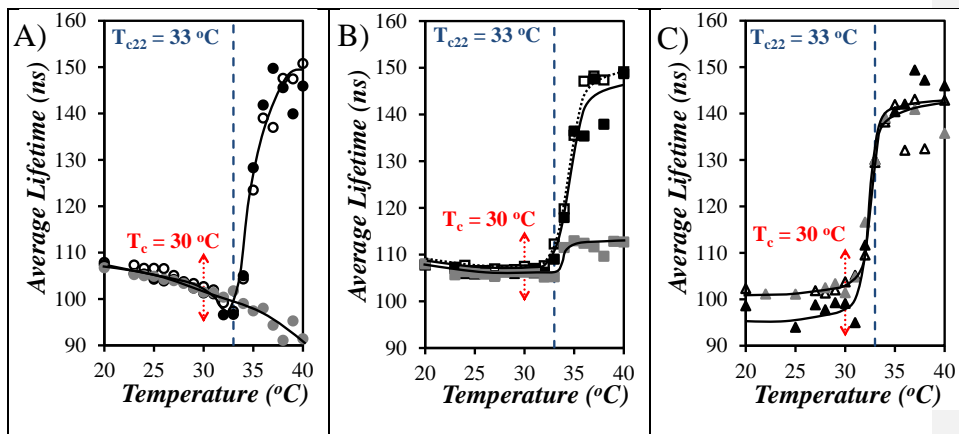


**Figure 8.** Plots of the number average lifetime of pyrene monomer decays for aqueous mixtures of Py<sub>1</sub>-PNIPAM and PNIPAM(22K) as a function of solution temperature. A) Py<sub>1</sub>-PNIPAM(7K), B) Py<sub>1</sub>-PNIPAM(12K), and C) Py<sub>1</sub>-PNIPAM(25K). Hollow symbols: 2<sup>nd</sup> heating ramp. Grey symbols: Py<sub>1</sub>-PNIPAM without a 10-fold excess of PNIPAM(22K).

***Comparison of the behavior of aqueous solutions of Py<sub>n</sub>-PNIPAM samples in the presence and absence of PNIPAM(22K):***

In Figure 9A, we present a schematic representation of the salient features of the demixing process of Py<sub>n</sub>-PNIPAM samples in water, with or without excess PNIPAM(22K), based on the evidence of LS, steady state and time-resolved fluorescence data reported here. Below  $T_{c22}$  PNIPAM(22K) does not interact with self-assembled Py<sub>n</sub>-PNIPAM. The situation changes when the solution temperature exceeds  $T_c(22)$  and PNIPM(22K) chains collapse and aggregate. Fluorescence data convincingly demonstrate that the environment of Py sequestered within Py<sub>n</sub>-PNIPAM mesoglobules changes as it becomes surrounded by a large excess of collapsed and partly dehydrated PNIPAM(22K) chains. The Py<sub>n</sub>-PNIPAM mesoglobules are sufficiently malleable around  $T_{c22}$  to allow the pyrene labels to diffuse as isolated entities away from the pyrene aggregates and invade the PNIPAM matrix enriched with collapsed PNIPAM(C22). This conclusion agrees

with that drawn from an earlier study of the mixing of pre-equilibrated mesoglobules of naphthalene- and pyrene-labeled PNIPAM which were found to undergo substantial mixing between 31 and 36 °C.<sup>33</sup> This earlier study revealed that mesoglobules pre-equilibrated at 40 °C did not merge, a point that cannot be detected in the current study focused on the early stages of mesoglobule formation and merging.

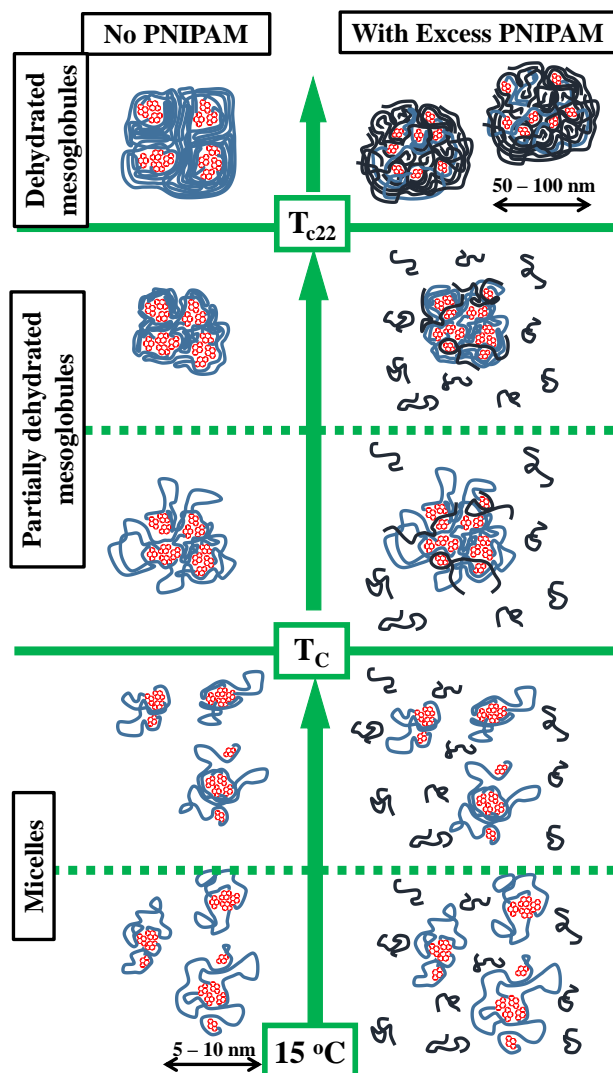


**Figure 9.** Schematic representation of the dehydration of the Py<sub>2</sub>-PNIPAM constructs in the absence (left) and the presence (right) of excess unlabeled PNIPAM. Color convention - Red: pyrene labels; light blue: PNIPAM chains linking two pyrene labels; dark blue: unlabeled PNIPAM. The solid green lines indicate the cloud points of the Py<sub>2</sub>-PNIPAM and

PNIPAM(22K), respectively. The two green dashed lines separate the state of the Py<sub>2</sub>-PNIPAM chains at the beginning and end of each regime.

The spinodal decomposition of most polymer solutions results in uncontrolled macroscopic phase separation. For a few water-miscible polymers, most notably PNIPAM, demixing from the aqueous phase at  $T_c$  generates stable mesoglobules with well-defined dimensions. This phenomenon attracts sustained experimental and theoretical attention.<sup>15–21,31–33</sup> H. Tanaka proposed that the unexpected stability of mesoglobules arises from the disparity between the long reptation time ( $\tau_{rep}$ ) required for chains to reptate from one mesoglobule to a colliding mesoglobule during the very short contact time ( $\tau_c$ ) between them.<sup>20,21</sup> This time is generally too short to secure anchoring points between the two mesoglobules that would eventually lead to their coalescence. The Py<sub>n</sub>-PNIPAM mesoglobules described here form stable mesoglobules at 35 °C in agreement with previous studies of hydrophobically-modified PNIPAM,<sup>27</sup> suggesting that the temperature region around 35 °C represents conditions where  $\tau_{rep} > \tau_c$ . Yet, the same mesoglobules readily coalesce with collapsed PNIPAM(22K) chains above  $T_{c22}$  (33 °C), which implies that the PNIPAM matrix of Py<sub>n</sub>-PNIPAM mesoglobules is sufficiently malleable to coalesce with collapsed PNIPAM chains.

To reconcile this phenomenon at odds with H. Tanaka's hypothesis, we consider that although the PNIPAM chains are not “frozen” in Py<sub>n</sub>-PNIPAM mesoglobules at temperatures between  $T_c$  and  $T_{c22}$ , the  $\tau_{repPy}$  for Py<sub>n</sub>-PNIPAM chains is much longer than  $\tau_{rep}$ , the reptation time of unlabeled PNIPAM. The hydrophobic pyrenes assembled within the mesoglobules act as physical crosslinkers and hinder chain motion. Such a phenomenon has already been recognized for hydrophobically modified PNIPAM mesoglobules.<sup>15</sup> While  $\tau_{repPy}$  for the Py<sub>n</sub>-PNIPAM mesoglobules is too long to enable the reptation of a Py<sub>n</sub>-PNIPAM chain into a

colliding PNIPAM(22K) mesoglobule,  $\tau_{\text{rep}22}$  for a PNIPAM(22K) chain in a non-fluorescent mesoglobule formed at  $T_{c22}$  and deprived of hydrophobic aggregates is expected to be much shorter than  $\tau_{\text{repPy}}$ . The shorter  $\tau_{\text{rep}22}$  would enable the reptation of PNIPAM(22K) chains into a  $\text{Py}_n$ -PNIPAM mesoglobule upon collision, followed by the formation of entanglements, the coalescence of the mesoglobules, and the dilution of the pyrene labels within the PNIPAM matrix. In turn this process would promote the disaggregation of the pyrene aggregates which would reduce  $\tau_{\text{repPy}}$  and further promote mesoglobule coalescence, thus resulting in the massive decrease in excimer formation described throughout this report.

## CONCLUSIONS

In summary, this study has established, first, that the  $\text{Py}_n$ -PNIPAM samples go through their cloud point at  $T_c$  ( $< T_{c22}$ ) and form mesoglobules that involve some mixing with PNIPAM(22K) in aqueous solution and, second, that the  $\text{Py}_n$ -PNIPAM mesoglobules are sufficiently malleable at temperatures above their respective cloud point to allow substantial mixing with PNIPAM(22K) above  $T_{c22}$ . Yet, the motion of the  $\text{Py}_n$ -PNIPAM chains is hindered by the hydrophobic pyrene aggregated within the  $\text{Py}_n$ -PNIPAM, which increases their reptation time, compared to the reptation time of PNIPAM(22K) chains. Although the  $\text{Py}_n$ -PNIPAM mesoglobules appear to be dynamically frozen, since the  $\text{Py}_n$ -PNIPAM mesoglobules do not coalesce above their respective  $T_c$  value (see Table 2), the PNIPAM chains connected to the pyrene labels remain sufficiently mobile to permit reptation of PNIPAM(22K) at  $T_{c22}$ . The dilution of the pyrene labels in the mixed mesoglobules decreases the local concentration of pyrene aggregates which progressively reduces  $\tau_{\text{repPy}}$  to  $\tau_{\text{rep}22}$ , at which point the pyrene labels are isolated inside the PNIPAM matrix of the mixed  $\text{Py}_n$ -PNIPAM/PNIPAM(22K) mesoglobules which are then expected to behave in the same manner as pure PNIPAM(22K) mesoglobules. In summary, this study represents a new illustration of the complex behavior of

PNIPAM mesoglobules which was identified by pyrene fluorescence and could be rationalized from the difference in  $\tau_{\text{rep}}$  values that exists between the hydrophobically modified and unmodified PNIPAM chains constituting their respective mesoglobules. In turn, such effects could be taken advantage of in the future to control the internal fluidity of mesoglobules made of hydrophobically modified thermoresponsive polymers, and thus their stability in solution, by adjusting the level of hydrophobic interactions taking place between the hydrophobes.

## ACKNOWLEDGEMENTS

The authors are thankful to NSERC for generous funding.

## SUPPORTING INFORMATION

Tables listing the pre-exponential factors and decay times of the monomer and excimer fluorescence decay analysis with sums of exponentials.

## REFERENCES

1. Heskins, M.; Guillet, J. E. Solution Properties of Poly(N-isopropylacrylamide). *J. Macromol. Sci.: A - Chem.* **1968**, *2*, 1441-1445.
2. Halperin, A.; Krüger, M.; Winnik, F. M. Poly(N-isopropylacrylamide) Phase Diagrams: Fifty Years of Research. *Angew Chem. Int. Ed.* **2015**, *54*, 15342-15367.
3. Duan, M.; Fang, S.; Guo, H.; Zhang, L. Viscometric Studies of Interactions between Hydrophobically Modified Acrylamide Copolymer and Poly(N-isopropylacrylamide) in Dilute Solutions. *J. Macromol. Sci. B Phys.* **2009**, *48*, 834-843.
4. Mylonas, Y.; Bokias, G.; Iliopoulos, I.; Staikos, G. Interpolymer Association Between Hydrophobically Modified Poly(sodium acrylate) and Poly(N-isopropylacrylamide) in

Water: the Role of Hydrophobic Interactions and Polymer Structure. *Eur. Polym. J.* **2006**, *42*, 849-857.

5. Yang, H.; Cheng, R.; Wang, Z. A Quantitative Analyses of the Viscometric Data of the Coil-to-Globule and Globule-to-Coil Transition of Poly(N-isopropylacrylamide) in Water. *Polymer* **2003**, *44*, 7175-7180.
6. Rinsdorf, H.; Venzmer, J.; Winnik, F.M. Interaction of Hydrophobically-Modified Poly-N-isopropylacrylamides with Model Membranes – or Playing a Molecular Accordion. *Angew. Chem. Int. Ed. Engl.* **1991**, *30*, 315-318.
7. Johnson, L. M.; Li, Z.; LaBelle, A. J. ; Bates, F. S. ; Lodge, T. P. ; Hillmyer, M. A. Impact of Polymer Excipient Molar Mass and End Groups on Hydrophobic Drug Solubility Enhancement. *Macromolecules* **2017**, *50*, 1102-1112.
8. Li, Z.; Johnson, L. M.; Ricarte, R. G. ; Yao, L. J. ; Hillmyer, M. A. ; Bates, F. S.; Lodge, T. P. Enhanced Performance of Blended Polymer Excipients in Delivering a Hydrophobic Drug through the Synergistic Action of Micelles and HPMCAS. *Langmuir* **2017**, *33*, 2837-2848.
9. Yip, J.; Duhamel, J.; Qiu, X. P.; Winnik, F. M. Fluorescence Studies of a Series of Monodisperse Telechelic  $\alpha,\omega$ -dipyrenyl Poly(N-isopropylacrylamide)s in Ethanol and Water. *Can. J. Chem.* **2011**, *89*, 163-172.
10. Chee, C. K.; Rimmer, S.; Soutar, I.; Swanson, L. Time-Resolved Fluorescence Anisotropy Studies of the Temperature-Induced Intramolecular Conformational Transition of Poly(N-isopropylacrylamide) in Dilute Aqueous Solution. *Polymer* **1997**, *38*, 483-486.
11. Kujawa, P.; Tanaka, F.; Winnik, F. M. Temperature-Dependent Properties of Telechelic Hydrophobically Modified Poly(N-isopropylacrylamides) in Water: Evidence from Light Scattering and Fluorescence Spectroscopy for the Formation of Stable Mesoglobules at Elevated Temperatures. *Macromolecules* **2006**, *39*, 3048-3055.



12. Lai, C.-T.; Chien, R.-H. ; Kuo, S.-W. ; Hong, J.-L. Tetraphenylthiophene-Functionalized Poly(*N*-isopropylacrylamide): Probing LCST with Aggregation-Induced Emission. *Macromolecules* **2011**, *44*, 6546-6556.
13. Niebuur, B.-J.; Claude, K.-L.; Pinzek, S.; Carker, C.; Raftopoulos, K. N.; Pipich, V.; Appavou, M.-S.; Schulte, A.; Papadakis, C. M. Pressure-Dependence of Poly(*N*-isopropylacrylamide) Mesoglobule Formation in Aqueous Solution. *ACS Macro Lett.* **2017**, *6*, 1180-1185.
14. Locatelli-Champagne, C.; Cloitre, M. Monitoring Mesoglobule Formation in PNIPAM Solutions Using Nile Red Solvatochromism. *Colloid Polym. Sci.* **2013**, *291*, 2911-2916.
15. Wu, C.; Li, W.; Zhu, X. X. Viscoelastic Effect on the Formation of Mesoglobular Phase in Dilute Solutions. *Macromolecules* **2004**, *37*, 4989-4992.
16. Gorelov, A. V.; Du Chesne, A.; Dawson, K. A. Phase Separation in Dilute Solutions of Poly(*N*-isopropylacrylamide). *Physica A* **1997**, *240*, 443-452.
17. Chuang, J.; Grosberg, A. Y.; Tanaka, T. Topological Repulsion Between Polymer Globules. *J. Chem. Phys.* **2000**, *112*, 6434-6442.
18. Dawson, K. A.; Gorelov, A. V.; Timoshenko, E. G.; Kuznetsov, Y. A.; Du Chesne, A. Formation of Mesoglobules from Phase Separation in Dilute Polymer Solutions: A Study in Experiments, Theory, and Applications. *Physica A* **1997**, *244*, 68-80.
19. Raos, G.; Allegra, G. A Cluster of Chains Can Be Smaller Than a Single Chain: New Interpretation of Kinetics of Collapse Experiments. *Macromolecules* **1996**, *29*, 8565-8567.
20. Tanaka, H. Unusual Phase Separation in a Polymer Solution caused by Asymmetric Molecular Dynamics. *Phys. Rev. Lett.* **1993**, *71*, 3158-3161.
21. Tanaka, H. Appearance of a Moving Droplet Phase and Unusual Networklike or Spongelike Patterns in a Phase-Separating Polymer Solution with a Double Phase-Shaped Phase Diagram. *Macromolecules* **1992**, *25*, 6377-6380.

22. Winnik, F. M. Photophysics of Preassociated Pyrenes in Aqueous Polymer Solutions and in Other Organized Media. *Chem. Rev.* **1993**, 93, 587-614.
23. Winnik, F. M.; Regismond, S. T. A. Fluorescence Methods in the Study of the Interactions of Surfactants with Polymers. *Colloids Surf. A* **1996**, 118, 1-39.
24. Pina, J.; Costa, T.; Seixas de Melo, J. S. In *Photochemistry*, Albini, A., Ed. 2011; Vol. 38, pp 67-109.
25. Duhamel, J. Pyrene-Labeled Water-Soluble Macromolecules as Fluorescent Mimics of Associative Thickeners. in *Fluorescence Studies of Polymer Containing Systems*; **2016**, Ed. Procházka, K.; Springer Series on Fluorescence.
26. Birks, J. B. Photophysics of Aromatic Molecules. Wiley: New York, 1970; pp. 301.
27. Fowler, M.; Duhamel, J.; Qiu, X. P. ; Korchagina, E. ; Winnik, F. M. Behaviour of the End-Groups of a Series of Pyrene End-Labeled Poly(*N*-isopropylacrylamide)s Probed by Time-Resolved Fluorescence. *MS accepted for publication in J. Polym. Sci.*
28. Yekta, A.; Xu, B.; Duhamel, J.; Adiwidjaja, H. ; Winnik, M. A. Fluorescence Studies of Associating Polymers in Water: Determination of the Chain End Aggregation Number and a Model for the Association Process. *Macromolecules* **1995**, 28, 956-966.
29. Hydrophilic Polymers: Performance with Environmental Acceptability; Glass, J. E.; Ed.; American Chemical Society: Washington, DC, 1996, Vol. 248.
30. Associative Polymers in Aqueous Solution: Glass, J. E., Ed.; American Chemical Society: Washington, DC, 2000, Vol. 765.
31. Aseyev, V.; Tenhu, H.; Winnik, F. M. Temperature-dependence of the colloidal stability of neutral amphiphilic polymers in water, in: Self-organization of amphiphilic copolymers in aqueous media, *Adv. Polym. Sci.* **2006**, 196, 1-85.
32. Zhang G. & Wu C. Folding and formation of mesoglobules in dilute copolymer solutions. *Adv. Polym. Sci.* **2006**, 195, 101–176.

33. Kujawa, P.; Aseyev, V.; Tenhu, H.; Winnik, F. M. Temperature-Sensitive Properties of Poly(*N*-isopropylacrylamide) Mesoglobules Formed in Dilute Aqueous Solutions Heated Above their Demixing Point. *Macromolecules* **2006**, *39*, 7686-7693.
34. Ding, H. ; Wu, F. ; Huang, Y. ; Zhang, Z. ; Nie, Y. Synthesis and Characterization of Temperature-Responsive Copolymer of PELGA Modified Poly(*N*-isopropylacrylamide). **2006**, *47*, 1575-1583.
35. Philipp, M.; Muller, U.; Aleksandrova, R.; Sanctuary, R.; Muller-Bushbaum, P.; Kruger, J. K. On the Elastic Nature of the Demixing Transition of Aqueous PNIPAM Solutions. *Soft Matter* **2012**, *8*, 111387-111395.
36. Koga, T.; Tanaka, F.; Motokawa, R.; Koizumi, S.; Winnik, F. M. Theoretical Modeling of Associated Structures in Aqueous Solutions of Hydrophobically Modified Telechelic PNIPAM Based on Neutron Scattering Study. *Macromolecules* **2008**, *41*, 9413-9422.
37. Yip, J.; Duhamel, J. ; Qiu, X. P.; Winnik, F. M. Long-Range Polymer Chain Dynamics of Pyrene-Labeled Poly(*N*-isopropylacrylamide)s Studied by Fluorescence. *Macromolecules* **2011**, *44*, 5363-5372.
38. Press, W. H.; Flannery, B. P.; Teukolsky, S. A.; Vetterling, W. T. *Numerical Recipes. The Art of Scientific Computing (Fortran Version)*; Cambridge University Press: Cambridge, 1992.
39. Siu, H.; Duhamel, J. The Importance of Considering Nonfluorescent Pyrene Aggregates for the Study of Pyrene-Labeled Associative Thickeners by Fluorescence. *Macromolecules* **2005**, *38*, 7184-7186.
40. Siu, H; Duhamel, J. Molar Absorbance Coefficient of Pyrene Aggregates in Water Generated by a Poly(ethylene oxide) Capped at a Single End with Pyrene. *J. Phys. Chem. B* **2012**, *116*, 1226-1233.

## Table of Content

